Fluorescently Labeled Gold Nanoparticles with Minimal Fluorescence Quenching

Yin Lu, Mita Dasog, Adam F. G. Leontowich, Robert W. J. Scott,* and Matthew F. Paige*

Department of Chemistry, 110 Science Place, University of Saskatchewan, Saskatoon, SK. S7N 5C9

Received: June 15, 2010; Revised Manuscript Received: September 2, 2010

Minimal quenching of fluorescence emission was observed when the fluorescent dye AlexaFluor 514 (AF514) was covalently bound to gold monolayer protected clusters (AuMPCs) that have negligible plasmon bands (diameters <2 nm). The fluorescence emission of the conjugated dye was measured as a function of dye−AuMPC mixing ratio with a combination of steady-state and time-resolved ensemble spectroscopic measurements in conjunction with single-molecule fluorescence microscopy. Fluorescence emission of the conjugated samples decreased slightly as a function of dye mixing ratio, which, in combination with a negligible change in fluorescence lifetime, was attributed to static quenching of the dye by the AuMPCs. From the single-molecule fluorescence measurements, it was observed that luminescent conjugates could still be detected, and, at all loading ratios, almost all of the dye−particle conjugates photobleached in either a single- or double-step process, with a small subpopulation exhibiting more than two photobleaching events. Beyond simple, irreversible photobleaching, no additional blinking dynamics were detected at the single-molecule level within the time resolution of the experiment. Emission intensities of coupled fluorophores were comparable with those measured of dye molecules that had not been attached to the AuMPCs, suggesting that the statically quenched fluorophores are entirely nonemissive, whereas the remaining dyes are essentially unquenched. These results are discussed in the context of other dye−AuMPC coupled systems described in the literature.

Introduction

The rapid development of nanotechnology over the past several decades has opened new possibilities for investigating interactions between photoexcited molecules and metal surfaces. When located in close proximity to metallic surfaces, photoexcited molecules can exhibit strong changes in electronic and optical properties, likely a result of the mixing of molecular and metallic electronic energy levels. Reports of both fluorescence quenching and emission enhancement have been reported in a wide range of metal−fluorophore conjugate systems (for a recent review see ref 1), along with extensive attempts to explain and model this behavior. While the majority of efforts to date have been directed at understanding spectroscopic behavior in planar systems (i.e., metallic films), there is an increasing interest in characterizing similar interactions between metal nanoparticles that are covalently linked with fluorophores, in part because of potential use of these systems for imaging, photoswitching, light harvesting, and biosensing applications.[2−4]

A common theme that has been observed in a number of covalently linked dye−AuMPC systems is a strong quenching of fluorescence emission upon dye coupling.[1,5−7] In some cases, fluorescence deactivation has been attributed to a combination of energy and electron transfer from the photoexcited species to the tethered particle,[1,8] as well as through coupling of the exciton into the surface plasmon band of the nanoparticle and radiative rate depression.[1,5,8,9] In other cases, the covalent linkage of organic moieties to AuMPCs (and nanostructured films) can affect optical properties of linked fluorophores through modulation of the surface plasmon absorption band of the particle, or by causing adjacent, linked fluorophore units to self-aggregate.[1,8,10,11] In still other situations, more subtle effects are important; for example, Jennings et al. have investigated the behavior of the molecular dye Cy5 coupled to 1.5 nm gold nanoparticles, and observed significant fluorescence quenching, as manifested by both a decrease in photoluminescence intensity and as a decrease in fluorescence lifetime.[12] These results were explained via a so-called nanosurface energy transfer (NSET) model, in which the photoexcited dye donates energy to the Au nanosurface according to a distance-dependent oscillator coupling ($1/d^4$, where d is the fluorophore−Au NP separation distance). These results are somewhat surprising as the surface plasmon resonance of 1.5 nm particles is weak (or nonexistent) and will not play a role in the energy transfer process, though the results can still be well rationalized through the intensity quenching mechanism described by Persson et al. for bulk metal films.[13]

In addition to standard ensemble electronic spectroscopy characterization tools, single-molecule fluorescence spectroscopy has also been demonstrated as a useful and insightful method for probing photoexcitation quenching in dye−AuMPC systems, as this approach allows detection of phenomena that are blurred by traditional ensemble averaging measurements.[14,15] In a seminal work in this area, Anger et al. modeled and systematically measured the dependence of fluorescence emission rate on the separation distance between laser-irradiated, 80 nm Au nanoparticles and individual dye molecules.[16] Both fluorescence enhancement (via local field amplification) and quenching (via nonradiative energy transfer) were observed in the same experiment, depending upon the Au nanoparticle−fluorophore separation. Cannone et al.[3] have explored the influence of coupling metal nanoparticles (diameters ranging from 5−20 nm) on the emission of a fluorescein derivative by single-molecule fluorescence spectroscopy. They observed complex millisecond time-scale fluorescence blinking dynamics for the dye−AuMPC system, which had a strong dependence on the size of the particles; average blinking on-times decreased with increasing particle diameters, whereas off-times increased with increasing particle diameter. They attributed the blinking dynamics to

* To whom correspondence should be addressed. E-mail: robert.scott@usask.ca (R.W.J.S.), matthew.paige@usask.ca (M.F.P.).

10.1021/jp105516f
Published on Web 09/20/2010

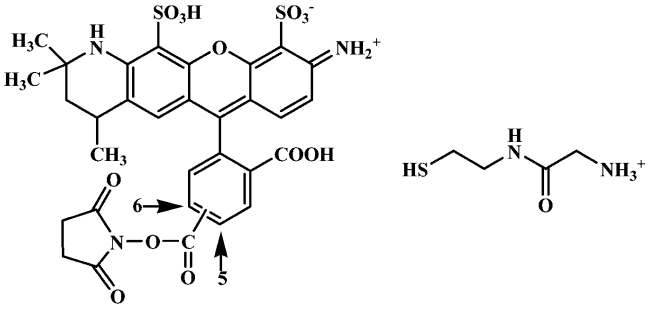

Figure 1. (A) Chemical structure of AF514 carboxylic acid, succinimidyl ester (mixed isomers with active ester on both position "5" and "6"). For subsequent figures, only the isomer with the active ester localized on position 5 will be shown. (B) Chemical structure of glycine-cysteamine.

energy coupling between the photoexcited fluorophore and the substantial plasmon features of the AuMPCs.

We seek to further explore photoexcitation quenching and energy transfer processes in covalently linked dye−AuMPC systems through a combination of ensemble and single-molecule fluorescence measurements. Of particular interest to these investigations is the role played by the AuMPC surface plasmon band in the quenching process; it might reasonably be anticipated that in smaller AuMPCs in which plasmon bands are vanishingly small (<2 nm), quenching should be substantially reduced, and at suitable dye−AuMPC separations, even negligible. It should be noted, however, that a recent time-dependent density functional theory study by Munoz-Losa et al.[17] has suggested that nonplasmonic particles may, in fact, be effective excitation energy transfer agents, and exploring this effect experimentally is of significant value. The synthesis and characterization of nearly monodisperse, water-soluble AuMPCs, in which the monolayer protection group is composed of glycine-cysteamine (Gly−CSA) has recently been described,[18,19] and these particles appear well suited for this purpose; the average composition of (Gly−CSA) MPCs employed in our study is $Au_{201}Gly{-}CSA_{71}$ with an average diameter of 1.8 ± 0.4 nm in diameter. Alex Fluor 514 (AF514, part A of Figure 1), an excellent fluorophore (high absorption cross-section, quantum yield, and comparatively low photobleaching quantum yield), which can be detected at the single-molecule level with excellent sensitivity, was chosen for preparing the dye-coupled MPCs. The fluorophores were linked to the AuMPCs through amide conjugation between the carboxylic group from dye molecules and the terminal free amine groups on the Au surface.

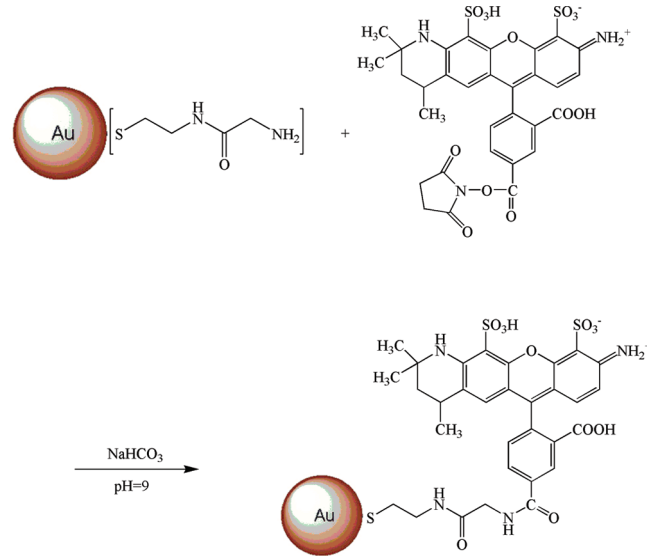

Figure 3. Schematic illustration of the conjugation reaction between Gly−CSA AuMPCs and AF514 carboxylic acid succinimidyl ester.

In this article, we describe the chemical synthesis and optical spectroscopic characterization of plasmon band free, labeled dye−AuMPC conjugates. By examining the spectroscopic properties of these labeled materials using a combination of steady-state and time-resolved methods, information about the extent of fluorescent-labeling, degree of fluorescence quenching, as well as the influence of the AuMPC on excited-state lifetime and single-molecule blinking dynamics has been obtained. Results are discussed in context of the recent literature and compared with those from closely related systems.

Experimental Section

Synthesis of Gly−CSA Protected AuMPCs. Synthesis of Gly−CSA protected AuMPCs was carried out as outlined in Figure 2, following established procedures previously reported by Leontowich et al.[19] From TEM and TGA investigations, the general composition of the AuMPCs was determined to be $Au_{201}(Gly{-}CSA)_{71}$, and mean particle diameters were 1.8 ± 0.4 nm.

Conjugation of Gly−CSA Au MPCs with AF514. The Gly−CSA AuMPCs were conjugated with AF514 carboxylic acid succinimdyl ester (Invitrogen) through the formation of an amide bond between the amine group on the Gly−CSA moiety and the carboxylic group of AF514 (structure shown in Figure 1).[18] Because formation of the amide bond is favorable

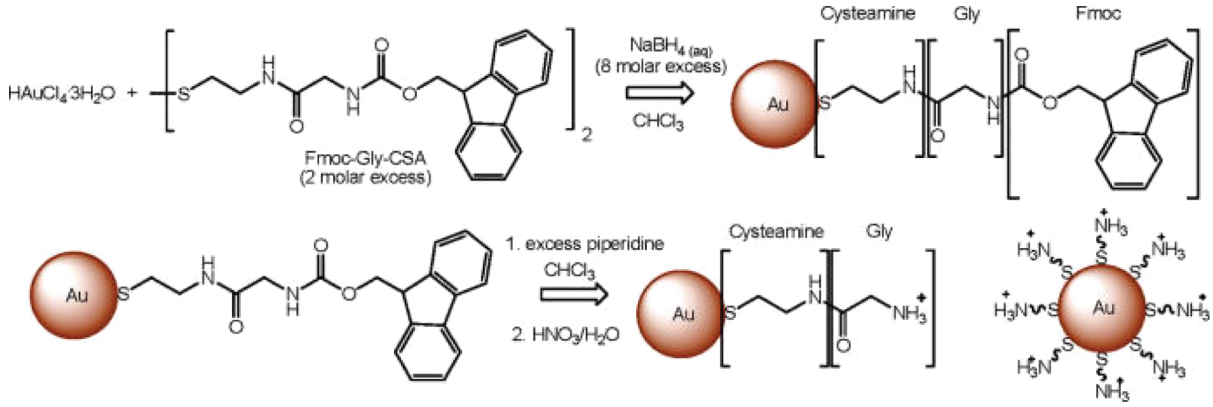

Figure 2. Synthetic preparation scheme for the Gly−CSA-functionalized AuMPCs.

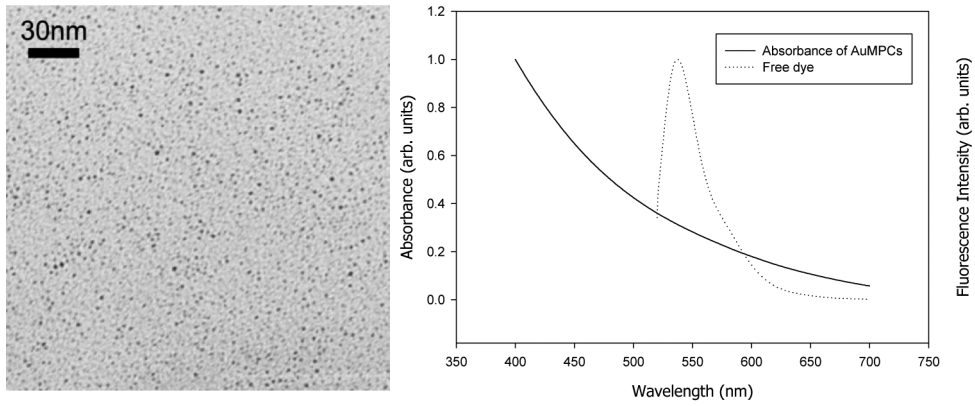

Figure 4. (A) Transmission electron micrograph of Gly−CSA functionalized AuMPCs and (B) extent of spectral overlap of the absorption spectra of AuMPCs and the emission spectra of AF514 (sample excited at 514 nm in order to reproduce imaging conditions used in subsequent single-molecule fluorescence microscopy experiments).

under slightly basic conditions, the AuMPCs were dissolved in a $NaHCO_3$ buffer solution (0.010 M, pH 9.0) to produce a 1.0 mg/mL stock solution. For all aqueous solutions, ultrapure water (Millipore, resistivity 18.2MΩ•cm) was used. The AF514 stock solution was prepared at a concentration of 1.40×10^{-4} M in DMSO. The dye to AuMPC mixing ratio was controlled by varying the volumes of the Gly−CSA AuMPC stock solution added to a fixed volume of dye solution. The $NaHCO_3$ buffer solution was then added to make a fixed total volume for all mixtures. The reactants were left stirring overnight under an N_2 atmosphere. Finally, the conjugates were dialyzed for 5 days against an acidic HNO_3 solution (pH 4.0) under N_2 to remove any unreacted dye.

Ensemble Spectroscopy Measurements. The emission spectra of Gly−CSA AuMPCs and AF514 mixtures at different mixing ratios were collected both before and after the conjugation reaction. The solutions were degassed with N_2, placed in quartz cuvettes and the emission spectra were measured on a PTI QuantaMaster Luminescence Fluorometer (Photon Technology International). The control samples were measured under the same conditions. Fluorescence lifetimes were measured using the method of time-correlated single-photon counting (TCSPC). Excitation was performed with the output from a mode-locked, frequency-doubled femtosecond Ti-sapphire laser at 492 nm, with an emission wavelength of 556 nm collected at the magic angle. Fluorescence decay profiles were fit using a nonlinear least-squares reconvolution procedure based on the Marquardt algorithm. The quality of fit was assessed through the value of the reduced χ^2 and through the distribution of weighted residuals.

Single-Molecule Epifluorescence Microscopy Measurements. After dialysis, the conjugates were diluted 100× with ultrapure water. Samples for single-molecule microscopy measurements were prepared by first spin-casting 120 μL of the diluted conjugate solution onto a cleaned glass coverslide, followed by a layer of dilute polymer (2% w/v poly(vinyl alcohol) in ultrapure water) to minimize the effect of oxygen-induced photobleaching of fluorescence. Control samples of AuMPCs that had not been mixed with AF514, as well as bare coverslides, coverslides that had been dosed with ultrapure water, and polymer coated coverslides showed no significant fluorescent impurities when examined under single-molecule imaging conditions.

For ensemble and single-molecule fluorescence imaging experiments, a home-built, wide-field epifluorescence microscope was used.[20] The output from a tunable argon-ion laser with a wavelength of 514 nm was passed through a spatial filter, collimated, and then focused by means of a 500 mm focal length lens onto the back focal plane of a 60×, 1.4NA oil-immersion objective lens (PlanApo, Nikon). Fluorescence emission from the sample was collected through two long-pass filters (540LP, Omega Optical) to remove residual excitation light and directed onto a wide-area, front-illuminated electron multiplying CCD camera (Cascade 512F, Photometrics). A data collection rate of 100 ms per frame was used.

Result and Discussion

Steady-State Absorption and Emission Spectra. Steady-state spectra of the unconjugated AuMPCs and AF514 were collected and are shown in Figure 4, along with a transmission electron micrograph taken from a typical sample of AuMPCs. Absorbance spectra of the AuMPCs consisted of a single, decreasing shoulder across the measured spectral range, with no additional spectral features present. The AuMPCs do not exhibit a characteristic plasmon resonance absorption band, as was anticipated from the particle size determined from electron microscopy (1.8 ± 0.4 nm). The emission spectrum of AF514 consisted of a single broad band (emission maximum of 537 nm), which is comparable with that provided by the manufacturer, except for a small blue shift (∼6 nm) in the emission maximum, which may be due to the slightly basic buffer solution used in these experiments. Given that AuMPCs with an average diameter that is less than 2 nm do not exhibit significant characteristic plasmon resonance absorption, the spectral overlap between the absorption of AuMPCs and the fluorescence emission is very limited. Thus, quenching of fluorescence emission due to coupling into the plasmon band is anticipated to be minimal.

Both absorption and emission spectra were collected for the dye−AuMPC particle conjugates prepared at different dye−AuMPC mixing ratios (moles of dye to moles of AuMPC; ratios adjusted by changing the amount of AuMPCs in the mixture). The absorbance spectra of the conjugates (not shown) were simply summations of the dye and AuMPC spectra without any additional features due to the conjugation reaction. Fluorescence emission spectra of the AF514 before and after conjugation were identical in shape and position of emission maxima, though a decrease in the overall fluorescence intensity was observed when increasing the concentration of AuMPCs in the mixture (shown in Figure 5). For comparison purposes, a series of emission

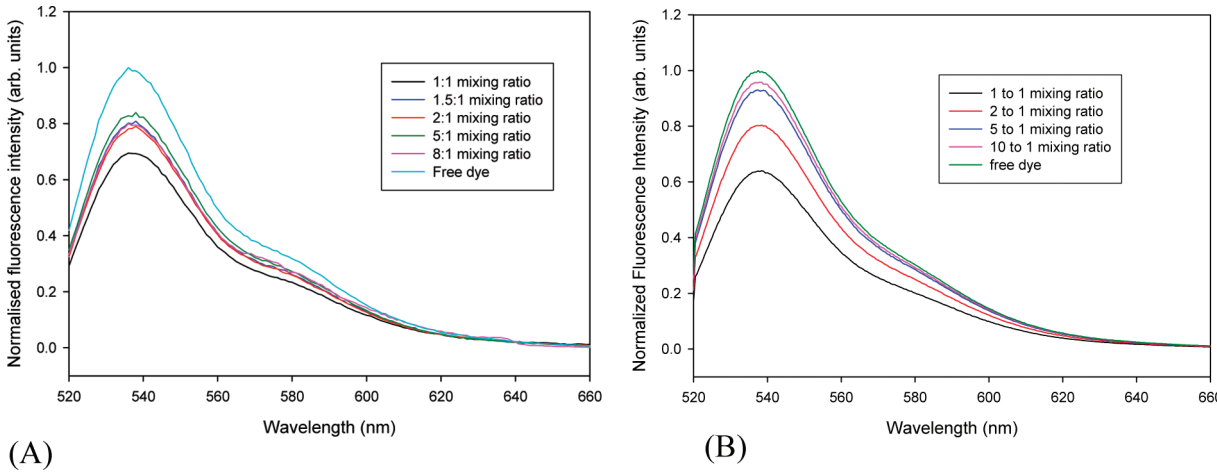

Figure 5. Fluorescence emission spectra showing fluorescence intensity as a function of the AF514 to Gly−CSA AuMPC mixing ratio: (A) immediately after mixing, and (B) after overnight conjugation.

spectra of mixtures of dye and AuMPCs immediately after mixing were collected and are also shown in Figure 5.

Comparison of parts A and B of Figure 5 indicates that there is little difference between the trends in fluorescence intensities of the AF514−AuMPC mixtures before and after the overnight conjugation period. This suggests that the conjugation reaction reaches completion shortly after mixing. However, the mixtures from both sets of reaction conditions do exhibit significantly lower fluorescence intensities in comparison with the dye alone, particularly at low dye to AuMPC mixing ratios. When the dye to AuMPC mixing ratio exceeds 2, the decrease in emission intensity that is caused by the presence of AuMPCs is negligible. This effect is explored in further detail, in conjunction with fluorescence lifetime measurements, in subsequent sections of this article.

Measurements were taken to examine the influence, if any, of free (unreacted) dye on the emission spectra of the mixtures through dialysis-based purification experiments. In these experiments, the dye to AuMPC mixing ratio was again adjusted by maintaining a fixed concentration of dye but changing the amount of AuMPCs in the mixture. After mixing, samples were extensively dialyzed to remove any unreacted dye. As a control experiment, a sample of free dye alone was also included. Emission spectra collected from the dialyzed mixtures and the control sample are shown in Figure 6. The fluorescence intensity of the mixtures decreased with increasing dye−AuMPC mixing ratio, which is the exact opposite of the observations from the unpurified conjugates. These results are consistent with only a small fraction of the fluorophores conjugating with the AuMPCs (typically around ∼1−5 fluorophores per AuMPC). That is, the majority of the dye that is mixed with the system does not react and is removed by dialysis; control samples of pure dye alone are only weakly fluorescent indicating that free dye is removed very efficiently. The decrease in fluorescence signal at high dye loading occurs because the majority of dye does not react with the particles and is removed by the purification step. The overall fluorescence signal is simply proportional to the quantity of labeled AuMPCs in the system, which increases with decreasing dye−AuMPC mixing ratio. While we cannot completely discount the possibility of low levels of desorbed Gly−CSA−dye linkages from the AuMPC surface (for recent reports of ligand exchange and desorption from AuMPCs see Ionita et al.[21,22]), we do note that the samples were synthesized, dialyzed, and examined under inert nitrogen atmosphere; previous work in our groups have shown that thiol desorption/oxidation on MPCs

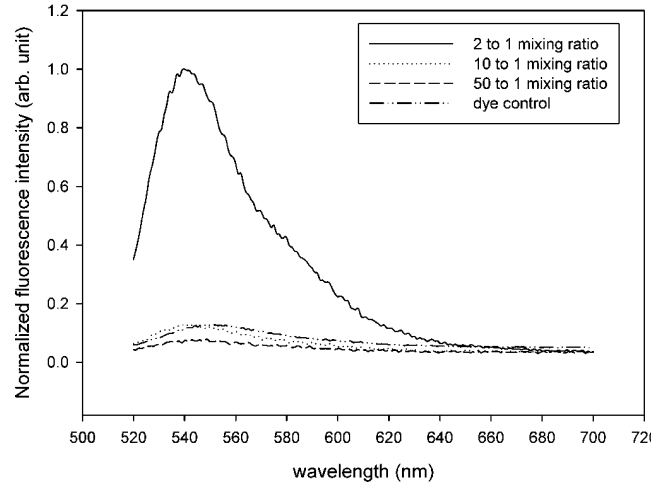

Figure 6. Fluorescence emission spectra for a series of dye−Au MPC mixtures and pure dye control sample after dialyzing for 5 days.

is more prominent in air and examinations of the Gly−CSA MPCs have shown that they are quite stable under inert atmosphere conditions.[19,23] Recent fluorescence correlation spectroscopy measurements by Navarro et al.[24] have been used to distinguish between desorbed dye molecules and those coupled with AuMPCs via determination of diffusion coefficients, and this approach might be of use in the future to quantify any contribution to the overall signal from desorbed dye.

Lifetime Measurement (TCSPC). To gain further insight into the spectral properties of AF514 after its conjugation with AuMPCs, fluorescence lifetimes of dye−AuMPC conjugates (mixing ratios ranging from 1:1 to 5:1) were measured. Control measurements were also carried out for the free dye prepared in buffer solution. As shown in Table 1, fluorescence lifetimes of the conjugates were measured after dialysis, and showed no significant difference in comparison with the free dye prepared in buffer solution. Both free dye and conjugate samples were well fit well by a double-exponential decay (eq 1) in which none of the fitting parameters (lifetimes or pre-exponential factors) were fixed.

$$I(t) = \alpha_1 e^{-t/\tau_1} + \alpha_2 e^{-t/\tau_2} \quad (1)$$

Curving fitting of all samples indicated the presence of two distinct components, a long-lived component with a lifetime of

TABLE 1: Fluorescence Lifetime Determined by Single- and Double-Exponential Decay Fits of the Fluorescence Decay Profiles of Samples Prepared at Different Dye−Au MPC Mixing Ratios

	Fitting parameters (two-component)				
Sample	α_1	τ_1 (ps)	α_2	τ_2 (ps)	χ^2
dye blank (buffer)	0.616	4086	0.384	157	1.09
dye/AuMPC (1:1)	0.585	4087	0.415	138	1.12
dye/AuMPC (1.5:1)	0.667	4072	0.333	173	1.23
dye/AuMPC(2:1)	0.475	4090	0.525	110	1.03
dye/AuMPC (5:1)	0.647	4079	0.353	173	1.00

4.0 ns and a short-lived component with lifetime of 0.1 ns. For conjugates with different dye−particle mixing ratios, the pre-exponential factors of both long-lived and short-lived species remain unchanged within our ability to measure: 60% of fluorophores decay with the long lifetime and the remaining 40% decay with short lifetime. These results are also comparable to the fitting data from the free dye samples prepared under the same solution conditions. We note that it is not immediately clear why all samples of AF514 (including the free dye) decay according to a two-component model; for a simple fluorophore in aqueous solution, a single-exponential decay is clearly the expected result. A number of chemical or photophysical effects may be at work here (e.g., aqueous equilibria, excited state processes, etc., for an example of another simple fluorophore system that shows multiexponential decay kinetics, see the work by Klonis[25]), though the presence of two components in the lifetime decay does not alter the principle result that the lifetimes are essentially unaltered by conjugation with the AuMPC.

The decrease in fluorescence intensity as a function of dye mixing ratio (Figure 5) is not trivial to reconcile with the lifetime data, as fluorescence quenching is often (though not always) associated with a change in the observed fluorescence lifetime. We can think of three possible mechanisms that give rise to this effect: (i) compensating changes in radiative and nonradiative decay rates, (ii) static quenching, and (iii) trivial inner filter effects. For case (i), the rate of fluorescence (k_f) can be written as a sum of radiative and nonradiative decay rates (k_{rad}, k_{nr}), and τ is the observed fluorescence lifetime:

$$k_f = \tau^{-1} = k_{rad} + k_{nr} \tag{2}$$

If conjugation of the fluorophore to the AuMPC resulted in changes to both decay rates that were approximately equal in magnitude but opposite in direction changes, then the net fluorescence intensity of the fluorophore could be decreased with negligible (within the ability to deconvolute) changes to the measured lifetime. It seems highly unlikely for such an exact, coincidental change to occur, however, and mechanisms (ii) and (iii) seem significantly more plausible.

Static quenching typically results from the formation of a nonfluorescent complex between fluorophore and quencher. Chemical species in systems exhibiting static quenching will be complexed with a quencher and nonemissive, or will not be complexed and emissive with a lifetime equal to that of the system in the absence of quencher.[26] In some cases, static quenching can be recognized through subtle changes in absorption spectra caused by formation of a quenched complex; as noted previously, we observed no changes in the absorption spectra (plotted on a linear energy scale to aid in comparison) upon conjugation. However, we have also performed a Stern−Volmer analysis to aid in mechanistic interpretation of the data. A standard Stern−Volmer analysis for simple static quenching indicates that quenching efficiency (ratio of fluorescence intensities for the quenched and unquenched system) should be linearly related to the quencher concentration [Q] (taken as the concentration of the AuMPCs):

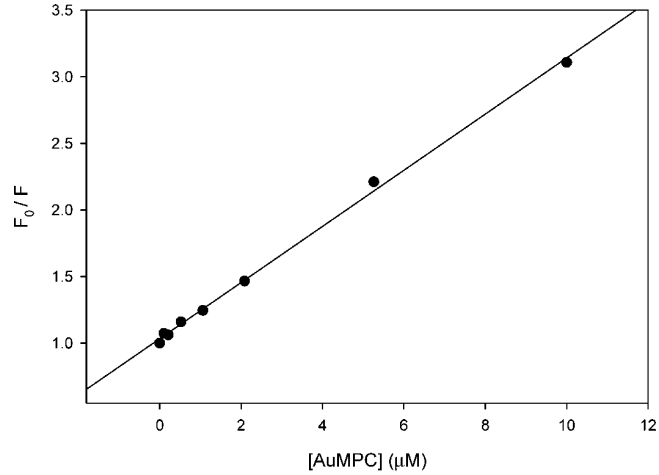

Figure 7. Stern−Volmer plot showing dependence of fluorescence quenching on concentration of AuMPCs, corrected for inner filter effects. The fitted static quenching constant is $K_s = 2.1 \times 10^5$ M^{-1}.

$$Q_{eff} = \frac{F_0}{F} = 1 + K_s[Q] \tag{3}$$

where F_0 and F are the fluorescence signal intensity for the unquenched and quenched species respectively, and K_s is the static quenching constant. To account for inner filter effects (photon reabsorption by the mixture components) we have applied the simple correction factor proposed previously by Lakowicz:[26]

$$F_{corrected} = F_{obs}C_1C_2 = F_{obs}10^{A_{ex}+A_{em}/2} \tag{4}$$

where F_x are the fluorescence intensities for the corrected and observed signals, C_1 and C_2 are the first- and second-order inner filter correction factors, and A_{ex} and A_{em} are the solution absorbances at the excitation and emission wavelengths, respectively. Figure 7 shows the Stern−Volmer plot using fluorescence intensities corrected with eq 4, along with a linear fit based on eq 3. Clearly, the data is very well represented by the static quenching model, suggesting that quenching in this system can be attributed to the formation of quenched complexes between the fluorophore and AuMPC. A static quenching constant of $K_s = 2.1 \times 10^5$ M^{-1} was calculated from the experimental data ($R^2 = 0.9979$).

It is of interest to compare the static quenching constant determined here with that obtained from a closely related system in which the fluorophore has not been covalently coupled to the particle. While it is difficult to find systems that are readily compared with the one described in this manuscript (particle sizes, compositions and fluorophores differ significantly), Cheng et al.[27] have reported on the quenching between tiopronin-decorated AuMPCs of a similar size to those reported here, and $[Ru(bpy)_3]^{2+}$ that was electrostatically associated with AuMPCs. Cheng et al. have reported static quenching constants of ~5.9 $\times 10^7$ M^{-1} for this system, with quenching constants increasing as a function of particle diameter. The approximately 2 orders

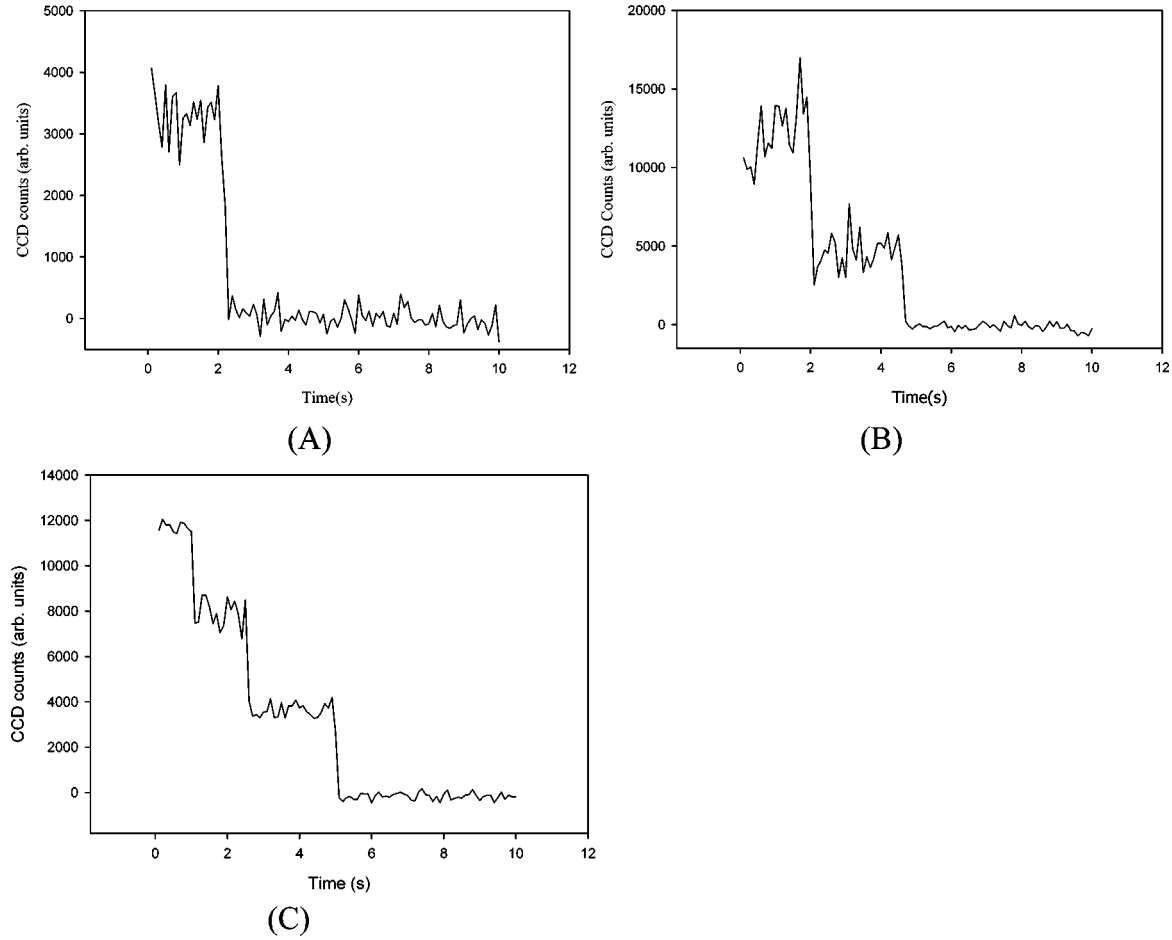

Figure 8. Representative fluorescence time trajectories of dye−AuMPC conjugates exhibiting (A) single-step photobleaching, (B) two-step photobleaching, and (C) three-step photobleaching collected by single-molecule microscopy (excitation intensity = 0.9 kW/cm^2 at 514 nm) of highly diluted ($\sim 10^{-8}$ M) samples.

of magnitude difference between quenching constants for comparable diameter particle suggests that the nature of the linker unit between fluorophore and AuMPC plays a crucial role in inhibiting quenching for the conjugated system. Presumably, for the quenched complex to form, the fluorophore and AuMPC must be in close proximity (and perhaps of the correct mutual orientation) and it seems highly likely that the short, rigid Gly−CSA linker hinders this association.

It is also worth noting that this result provides direct experimental support of the work by Munoz-Losa et al., in which it is suggested that effective excitation energy transfer between fluorophores and AuMPCs does not necessarily require the existence of surface plasmons, and, in some situations, can take place with comparable efficiency.[17] While the significant differences between the experimental system explored here and that described by Munoz-Losa (particle shape, nature of the fluorophore, separation, and geometry of fluorophore−quencher pair) preclude quantitative comparison, the qualitative agreement between the two approaches is excellent and highlights the importance of nonplasmonic particles when considering excitation energy transfer processes.

To summarize the results of the ensemble spectroscopy experiments, the measurements indicate that the conjugated fluorophores exist in one of two states: efficiently quenched through interaction with the AuMPCs or strongly emissive. The remainder of this investigation makes use of single-molecule fluorescence measurements to provide further evidence that this is the case.

Single-Molecule Fluorescence Microscopy. To further explore the influence on fluorophore emission played by conjugation to Au MPCs, single-molecule fluorescence measurements were carried out via epifluorescence imaging of highly diluted ($\sim 10^{-8}$ M) dye−particle conjugates deposited on glass coverslips. Images consisted of a series of discrete, brightly luminescent entities on a dark background, with the entities having diameters that were comparable to the diffraction limit of the excitation light ($\sim$300 nm). Because of the rigorous control experiments described in the Experimental Section, in combination with the fact that all of the dye−AuMPC conjugates had undergone extensive dialysis (the efficacy of which was demonstrated earlier in this manuscript) followed by 100-fold dilution in pure solvent, all of the fluorescent entities that were imaged could reasonably be attributed to AF514 molecules that were covalently bound to the AuMPCs. On a few occasions, extremely bright entities that were considerably larger than the $\sim$300 nm diffraction limited size were observed. The source of these unusually large, emissive entities is currently unclear, though they likely consist of aggregated AuMPCs. These entities were excluded in subsequent data analysis.

In conventional single-molecule imaging experiments, fluorophores typically exhibit single-step photobleaching in their fluorescence time trajectories (integrated fluorescence emission intensity as a function of time) upon continuous illumination, as expected from the photodegradation of a discrete emitter.[15] For the systems studied here, fluorescence time trajectories that contained both individual photobleaching steps, as well as

TABLE 2: Percentage Distributions in Number of Step in Photobleaching As Determined by Epifluorescence Microscopy for the 1:1, 1.5:1, 2:1, 5:1 Dye−AuMPC Mixing Ratio Samples, As Well as a Free Dye Control Sample

dye/AuMPCs	single step	two step	three step	four step
1 to 1	53%	43%	4%	0%
1.5 to 1	48%	48%	4%	0%
2 to 1	57%	40%	3%	0%
5 to 1	45%	46%	8%	1%
free dye	91%	9%	0%	0%

multiple, sequential photobleaching steps were observed. Several representative time trajectories that show the different types of photobleaching are shown in parts A−C of Figure 8 (single-step, two-step, and three-step photobleaching). It should be noted that the entities exhibited negligible repeated on−off blinking within the time resolution of the experiment, an effect that has been observed in a number of other single-molecule systems (see[28] for example), regardless of the number of photobleaching steps. After a fluorophore underwent photobleaching, it was permanently nonemissive.

Fluorescence time-trajectories were classified into four different subgroups according to the number of discrete photobleaching steps they exhibited (samples having one, two, three, and four well-defined steps were observed). The fraction of the total measured samples (over 200 particles measured per group) in each subgroup is summarized in Table 2 for four different dye−AuMPC loading ratios and the free dye alone. As shown in Table 2, at low dye-loading ratios, approximately >90% of the sample population photobleached in either a single or double step, with single-step photobleaching occurring slightly more frequently than double-step (a small fraction of free dye molecules showed two steps, but the vast majority photobleached in a single step). The remaining ∼3−4% of the population photobleached in three discrete steps. As the dye-loading ratio was increased, there was a slight shift in favor of the formation of the double-step photobleaching, and at the 5:1 dye−AuMPC ratio, the three-step photobleaching frequency

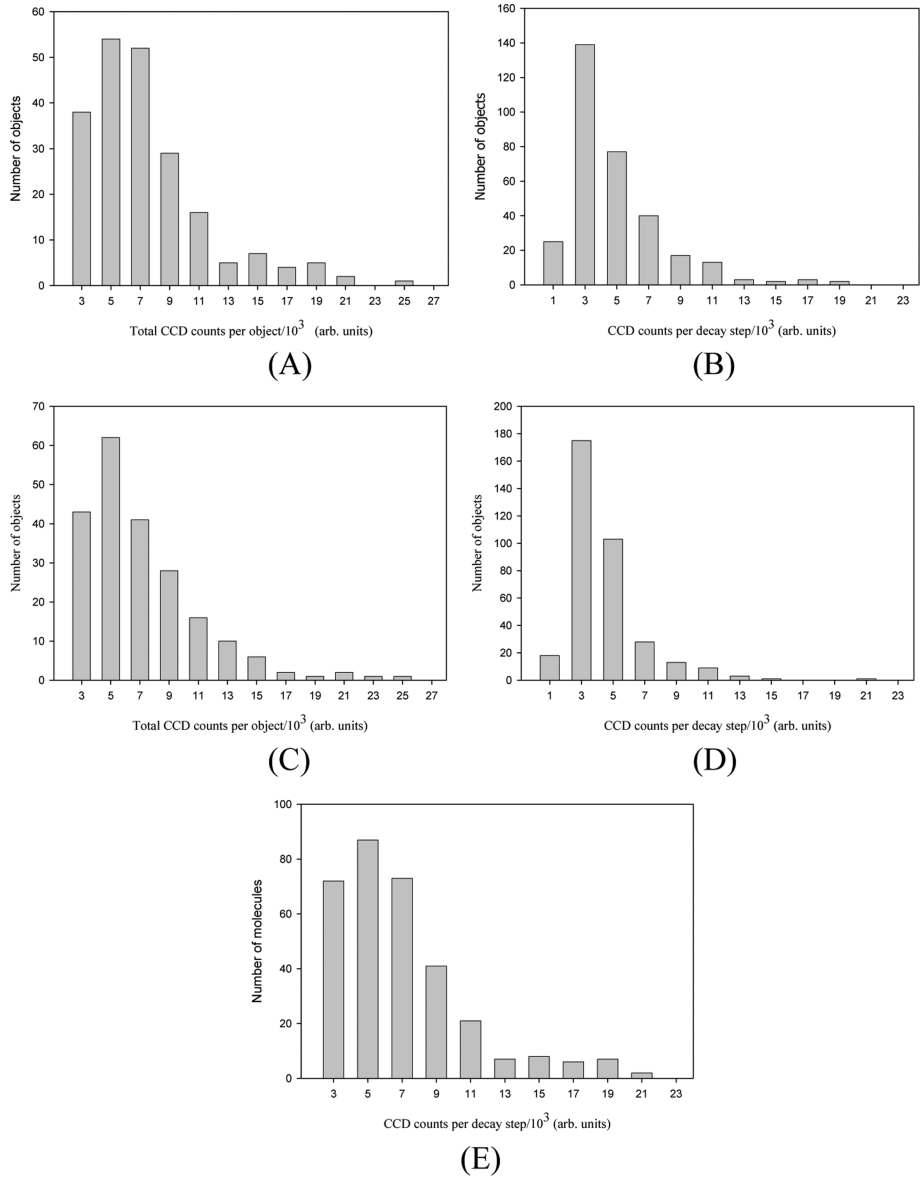

Figure 9. Histograms of fluorescence intensities from single-molecule measurements. (A) Total fluorescence intensity for entire entity, 1:1 dye-loading ratio, (B) fluorescence intensity of individual photobleaching steps, 1:1 dye-loading ratio, (C) total fluorescence intensity for entire entity, 5:1 dye-loading ratio, (D) fluorescence intensity of individual photobleaching steps, 5:1 dye loading ratio, (E) AF514 dye. (Excitation intensity in all cases was 0.9 kW/cm^2 at 514 nm).

increased. Four-step photobleaching was only observed in samples prepared with this higher dye-loading ratio. The results of these single-molecule measurements are in excellent general agreement with the ensemble results, which indicated the average coordination number of dye on each Au particle is between 1 and 2. While the use of higher dye-loading ratios resulted in a slight increase in the number of AuMPCs that were labeled with more than two fluorophores, the effect was quite small, indicating that saturation of the available conjugation sites had already occurred. The number of dye molecules that can be covalently bound to the AuMPC is surprisingly low, given that the entire particle surface is functionalized with reactive amine groups and an excess of reactive dye was used in the chemical synthesis. Of course, a fraction of the bound dye molecules will be statically quenched and nonemissive, but the combination of ensemble and single-molecule measurements provides compelling evidence that there is simply a small number of dye molecules bound to the AuMPCs. It seems plausible that the small particle diameters in combination with the relatively bulky fluorophore (long axis of the AF514 fluorophore is ~1.8 nm, as determined by MMFF molecular modeling calculations, *Spartan '08*) results in significant steric crowding, making the coupling of more than a few fluorophores problematic.

To further elucidate the influence of the AuMPC on fluorophore emission and to explore the nature of the static quenching process at the single-molecule level, an analysis of single-molecule fluorescence intensities of the photobleaching steps was carried out. Figure 9 shows histograms of fluorescence intensities taken from two dye-loading ratios, 1:1 to 5:1 (results from intermediate dye-loading ratios were comparable). Because of the appearance of multiple photobleaching steps, analysis of both the total fluorescence intensity of the entire entities, as well as the fluorescence intensity of each individual decay step in the multistep decays was carried out. Serving as a reference, the fluorescence intensity distributions of monomer AF514 were also measured under the same imaging conditions, and are included in Figure 9 for comparison. As seen via the histograms, the total fluorescence intensity showed minimal changes as a function of dye loading, indicating that the average compositions of the dye−particle conjugates are similar for all ratios. Again, this is the expected result from the ensemble measurements, which showed that only a small number of fully fluorescent molecules (~1−2) are present, regardless of the amount of dye used in the coupling reaction. The fluorescence intensity of the photobleaching steps also showed negligible differences between samples prepared at different dye-loading ratios, nor was there any indication that the fluorescence intensity of any individual photobleaching step in the multiple bleaching event decay curves varied significantly from the others. We interpret these results to mean that the fluorescence intensities of individual dye molecules bound to the AuMPC were essentially independent of the amount of dye present.

It should be noted that there was a small but detectable difference in terms of fluorescence intensity between the pure dye control sample and dye-conjugated samples, with the mean fluorescence intensity of the control sample being marginally greater than that measured for the AuMPC-coupled fluorophores (mean ~4800 CCD counts/100 ms versus ~4500 CCD counts/100 ms). At present, it is difficult to rationalize this small difference in emission intensity with the available data; certainly, the ensemble data indicates that the small changes in fluorescence emission is from static quenching, and as such, we expected the individual molecules to exhibit the same fluorescence emission intensity as that measured for the coupled dye molecules. It is possible that there are purely single-molecule effects at work that cannot readily be detected using the relatively simple epifluorescence microscope system used in these experiments. Spectral wandering, for example, shifts in fluorescence emission spectra that are often seen in single-molecule experiments, could result in significant movement of the emission spectrum to shorter wavelengths where the optical filters of the microscope act to reduce net fluorescence signals. Subtle changes to fluorescence lifetime might also be taking place, though at present, limitations in instrumentation prevent us from probing these effects further. Efforts to refine our instrumental setup an enable these measurements at the single-molecule level are ongoing.

Conclusions

The fluorescent molecule AF514 was covalently coupled to monodisperse, 1.8 nm diameter AuMPCs, and the optical spectroscopy properties of the dye−AuMPC conjugate were examined through a combination of ensemble and single-molecule fluorescence measurements. It was observed that after coupling, the AF514 exhibits only minimal fluorescence quenching, with the reduced fluorescence intensity attributed to static quenching of some fraction of AuMPC-bound fluorophores in conjunction with self-absorption (inner filter) effects. Only a small number of fluorophores could be coupled to the AuMPCs, because the size of the AF514 molecules are comparable to that of the AuMPCs and steric hindrance prevents greater extents of dye loading. Single-molecule measurements verified these observations, with fluorescence time trajectories consisting of either single- or multiple-step sequential photobleaching, corresponding to the photobleaching of a small number of discrete, but strongly emissive fluorophores tethered to the AuMPC surface. The results in combination indicate that there are two populations of tethered fluorophores on the AuMPC surface, those that are efficiently quenched through interaction with the AuMPCs, and a separate population that remains strongly emissive and essentially unquenched.

Acknowledgment. Funding for this work was provided by the Natural Sciences and Engineering Research Council of Canada (NSERC), the Canada Foundation for Innovation (CFI), the Province of Saskatchewan and by the University of Saskatchewan. The Saskatchewan Structural Sciences Centre and Professor Ron Steer are acknowledged for providing access to the TCSPC equipment, and Dr. Sophie Brunet is thanked for providing assistance with lifetime measurements. Christina Calver is thanked for providing assistance with chemical synthesis.

References and Notes

(1) Thomas, K. G.; Kamat, P. V. *Acc. Chem. Res.* **2003**, *36*, 888.
(2) Aslan, K.; Perez-Luna, V. H. *Journal of Fluorescence* **2004**, *14*, 401.
(3) Cannone, F.; Chirico, G.; Bizzarri, A. R.; Cannistraro, S. *J. Phys. Chem. B* **2006**, *110*, 16491.
(4) Chhabra, R.; Sharma, J.; Wang, H. N.; Zou, S. L.; Lin, S.; Yan, H.; Lindsay, S.; Liu, Y. *Nanotechnology* **2009**, *20*, 485201.
(5) Mayilo, S.; Kloster, M. A.; Wunderlich, M.; Lutich, A.; Klar, T. A.; Nichtl, A.; Kurzinger, K.; Stefani, F. D.; Feldmann, J. *Nano Lett.* **2009**, *9*, 4558.
(6) Nerambourg, N.; Werts, M. H. V.; Charlot, M.; Blanchard-Desce, M. *Langmuir* **2007**, *23*, 5563.
(7) Pons, T.; Medintz, I. L.; Sapsford, K. E.; Higashiya, S.; Grimes, A. F.; English, D. S.; Mattoussi, H. *Nano Lett.* **2007**, *7*, 3157.
(8) Adams, D. M.; Brus, L.; Chidsey, C. E. D.; Creager, S.; Creutz, C.; Kagan, C. R.; Kamat, P. V.; Lieberman, M.; Lindsay, S.; Marcus, R. A.;

Metzger, R. M.; Michel-Beyerle, M. E.; Miller, J. R.; Newton, M. D.; Rolison, D. R.; Sankey, O.; Schanze, K. S.; Yardley, J.; Zhu, X. Y. *J. Phys. Chem. B* **2003**, *107*, 6668.

(9) Dulkeith, E.; Ringler, M.; Klar, T. A.; Feldmann, J.; Javier, A. M.; Parak, W. J. *Nano Lett.* **2005**, *5*, 585.

(10) Ipe, B. I.; Thomas, K. G.; Barazzouk, S.; Hotchandani, S.; Kamat, P. V. *J. Phys. Chem. B* **2002**, *106*, 18.

(11) Kamat, P. V.; Barazzouk, S.; Hotchandani, S. *Angew. Chem., Int. Ed.* **2002**, *41*, 2764.

(12) Jennings, T. L.; Singh, M. P.; Strouse, G. F. *J. Am. Chem. Soc.* **2006**, *128*, 5462.

(13) Persson, B. N. J.; Lang, N. D. *Phys. Rev. B* **1982**, *26*, 5409.

(14) Moerner, W. E.; Fromm, D. P. *Rev. Sci. Instrum.* **2003**, *74*, 3597.

(15) Moerner, W. E.; Orrit, M. *Science* **1999**, *283*, 1670.

(16) Anger, P.; Bharadwaj, P.; Novotny, L. *Phys. Rev. Lett.* **2006**, *96*.

(17) Munoz-Losa, A.; Vukovic, S.; Corni, S.; Mennucci, B. *J. Phys. Chem. C* **2009**, *113*, 16364.

(18) Dasog, M.; Kavianpour, A.; Paige, M. F.; Kraatz, H. B.; Scott, R. W. J. *Can. J. Chem.* **2008**, *86*, 368.

(19) Leontowich, A. F. G.; Calver, C. F.; Dasog, M.; Scott, R. W. J. *Langmuir* **2010**, *26*, 1285.

(20) Bagh, S.; Paige, M. F. *J. Phys. Chem. A* **2006**, *110*, 7057.

(21) Ionita, P.; Volkov, A.; Jeschke, G.; Chechik, V. *Anal. Chem.* **2008**, *80*, 95.

(22) Ionita, P.; Wolowska, J.; Chechik, V.; Caragheorgheopol, A. *J. Phys. Chem. C* **2007**, *111*, 16717.

(23) Dasog, M.; Scott, R. W. J. *Langmuir* **2007**, *23*, 3381.

(24) Navarro, J. R. G.; Plugge, M.; Loumaigne, M.; Sanchez-Gonzalez, A.; Mennucci, B.; Debarre, A.; Brouwer, A. M.; Werts, M. H. V. *Photochem. Photobiol. Sci.* **2010**, *9*, 1042.

(25) Klonis, N.; Sawyer, W. H. *Photochem. Photobiol.* **2003**, *77*, 502.

(26) Lakowicz, J. *Principles of Fluorescence Spectrosopy*, 2nd ed.; Kluwer Academic: New York, 1999.

(27) Cheng, P. P. H.; Silvester, D.; Wang, G. L.; Kalyuzhny, G.; Douglas, A.; Murray, R. W. *J. Phys. Chem. B* **2006**, *110*, 4637.

(28) Clifford, J. N.; Bell, T. D. M.; Tinnefeld, P.; Heilemann, M.; Melnikov, S. M.; Hotta, J.; Sliwa, M.; Dedecker, P.; Sauer, M.; Hofkens, J.; Yeow, E. K. L. *J. Phys. Chem. B* **2007**, *111*, 6987.

JP105516F